Application of carbon-tungsten, carbon-beryllium and carbon-aluminium nanostructures in divertors coatings from fusion reactor

V. CIUPINA[a,c,d], I. MORJAN[b], R. VLADOIU[a], C. P. LUNGU[b], C. POROSNICU[b], I. JEPU[b], G. PRODAN[a,d], I. M. STANESCU[a], A. MANDES[a], M. CONTULOV[a], V. DINCA[a], M. PRODAN[a], V. NICOLESCU[e]
[a]*University of Constanta, Mamaia Avenue 124, Constanta, 900527, Romania*
[b]*National Institute for Laser Plasma and Radiation Physics, Magurele, 077125, Romania*
[c]*Academy of Romanian Scientists*
[d]*Institute for nanotechnologies and renewable energies*
[e]*CERONAV , 69A Pescarilor Str., Romania*

Carbon fiber composites (CFCs) are currently used in current ITER design. The strike point zone area is covered by tungsten based CFCs tiles. Beryllium based CFCs are use in other parts of divertor region. Those materials are a compromise based on experience with individual materials in many different tokamaks. Also aluminum CFCs can be a candidate material for the First Wall in ITER. We see that TVA method is suitable for the synthesis of wide range of materials, and more important is a low cost method that allow variation of concentration in one shot deposition. We compare CFCs nanostructures (Al, Be, W) by modeling and simulated TEM images, and also by evaluate the response of generated structure under ions bombardements. TEM comparative studies show that Al and Be CFCs contrast of images are verry closed to each other. Better contrast are obtain for W-CFCs. Ion bombardments shows same conclusion, Al and Be exibits the same behavior under ions bombardments. We estimate the energy limit of deffects apparition from stoping range versus energy graphics. The energy of defects apparition are close for Be and Al, between 500-1000ev and larger than 1000eV for W-CFCs. The Michelson contrast evaluated from TEM images show a similar value for Al and Be, but increased for W-CFCs.

(Received Decembrie 3, 2012; accepted November 7, 2013)

Keywords: Carbon composite, Simualtion, Tokamaks, TEM, Stoping range

1. Introduction

Carbon fiber composites (CFCs) are currently used in current ITER design. The strike point zone area is covered by tungsten based CFCs tiles. Beryllium based CFCs are use in other parts of divertor region. Those materials are a compromise based on experience with individual materials in many different tokamaks [1,2,3,4]. Also aluminum CFCs can be a candidate material for the First Wall in ITER.

As shown in previous papers [5,6], beryllium CFCs and tungsten CFCs have the physical properties that made them a good choice to cover tiles in ITER first wall. Nanostructured CFCs was obtained using the thermionic vacuum arc method (TVA) in two electronic guns configuration. The growing thin film are maintained under plasma ions bombardment during deposition with controls over the energy of those ions. The externally heated cathode are used to generate thermoelectrons, focused further by means of Wehnelt cylinder and accelerate towards anode whose material is evaporated and under a high voltage DC supply bright plasma are ignited.

The beryllium and aluminium nanoparticles ignite at low temperature and depend mainly of morphological properties. The layer of beryllium nanoparticles with 1-5μm diameter can be ignited between 540ºC and 700 ºC [7]. A cloud formed by 1μm beryllium nanoparticles ignite at 910 ºC. Ignition temperature are between 300-600 ºC for aluminium layer, and 650-700ºC for cloud aluminum powder. Another infringement are toxicity, beryllium are rated as potential carcinogens, and must be label properly [8]. Aluminum and tungsten materials are not labeled so.

Related to physical properties, the melting point of bulk aluminum are 627ºC below beryllium, and aluminum hardness is half of beryllium [9]. Our goals are to exchange, if it's possible, the C-Be thin films, with equivalent C-Al thin films. For this, we need a solution for material synthesis and also find correct concentrations between carbon and aluminum. We see that TVA method is suitable for the synthesis of wide range of materials [10, 11, 12], and more important is a low cost method that allow variation of concentration in one shot deposition.

2. Experimental

The experimental setup (Figure 1) of TVA method was modified so we can varies de M/C report (with M=W, BE, Al). Additional source was added to setup, that allow simoultaneous deposition of multiple components. Also,

we can controls deposition order by activate corresponded source. The anod-anod distance was 20 cm and target-anod distance was 25 cm. These configuration allow a variation of particle flux in each target, that depend on gemetrical future: distance and angle. Concentration of final structure is proportional with position of target substrates. Electron beam from heated filements evaporate M and C used as anode, by applied a high voltage between anodes and cathodes. We obtain a simultaneous bright plasma of M and C. To obtain recquired concentration we can control each plasma by electron beam intensities and applied high voltage. For target substrate we used Si and graphite and target ansamble was mantained at 675K degree to eliminate thermal shock due to interactions of plasma ions with target, and minimize apparition of deffects from mechanical stress.

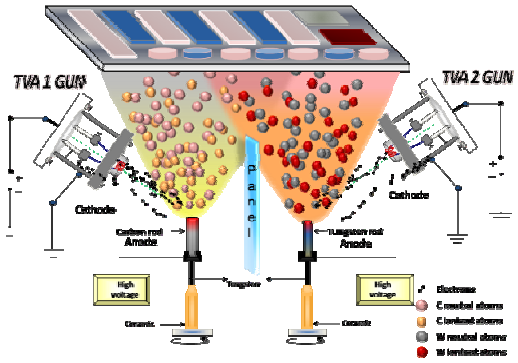

Fig. 1. Schematics of single and double source TVA geometry.

The TVA goals are to evaporate the neutral atoms with such a rate so to provide a high vapor density of neutrals atoms. The electron beam is power enough to ensure a sufficient high charge carrier production to compensate the continuous loss of charge. Thin film is condensing exclusively from the plasma state of the material to be deposited without any other buffer gas and without droplets. In some operating conditions the plasma source produce energetic ions without any additional ion acceleration means like acceleration grids or polarization systems. The deposition rate could be easily controlled and even higher that other methods of deposition**.** It is possible to control the energy of ions during the deposition process.

The TVA steps consist in: a). Generates a gas - free and macroparticle-free plasma in material vapors with a degree of ionization up to 20%. b). Specific means to accelerate the ions like grids are not necessary. c). in the sputtering case and d). Offers the possibility to adjust the directed energy of the ions by controlling operating parameters

C-M thin films was obtained using a double source configuration, one for atomize carbon rods, and second for aluminum powder. The resulted thin film was studies with SEM, EDS, TEM and tribological method, to obtain information about morphology, crystalline structure, and physical properties. Those properties were compared with reported values obtained for M-C films. SEM (Figure 2) and EDS studies were performed on a Philips ESEM200 microscope at different magnification (500x, 1000x, and 10000x). TEM images were obtained on Philips CM120ST with Megaview III CCD camera with sample prepared by scratch method. For morphological characterization we assume a lognormal distribution of measured sizes of identified nanoparticles and Feret diameter to estimate those sizes. The experimental histogram was fit with user build lognormal function in SCIDavis application. Crystalline structure was found using electron diffraction pattern, measured in CRISP2, ELD for polycrystalline materials and manually indexing with analytical procedure. The lattice parameters were estimate using Cohen method with modified Nelson-Riley function.

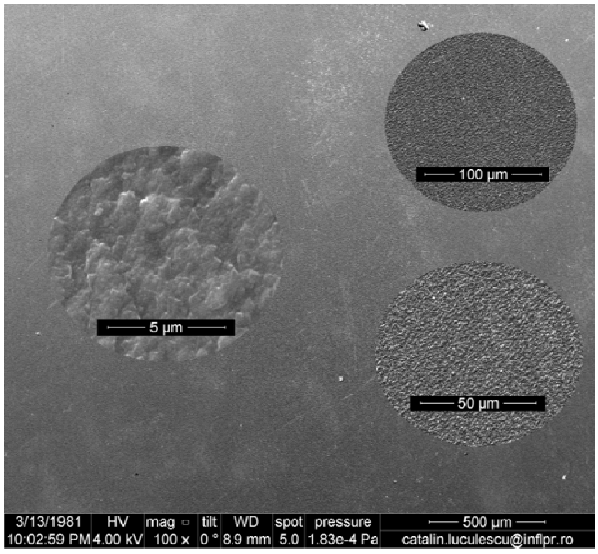

Fig. 2. SEM image of Al-CFCs.

For W-CFCs we obtain from electron diffraction, most intense line at 0.330 nm(002C), 0.218 nm (100C/110W), 0.191 nm (101C), 0.176 nm (102C), 0.125 nm (110C/112W) and 0.112 nm (105C/220W), indexed with graphite hexagonal structure [13] and tungsten cubic structure [14]. Assuming a lognormal distribution for crystallite dimension we found ~4 nm for mesured Feret

diameter on TEM image and from electron diffraction pattern by means of Debye-Scherrer relation for most intense lines, we found a mean value of ~3.3 nm. The C-Be film has the caracteristics of polycristalline materials, with grain size around 14 nm and the most four intense lines can be indexed with hexagonal structure of Be (P6(3)/mc a=0.229nm and c=0.358nm [15]). Using Debye-Scherrer relation we found an mean crystallite size of 8.6 nm. The most intense peak was found at 0.197nm Be(100), 0.173nm Be(101), 0.133nm Be(102) and 0.114nm Be(110) with mean relative error ~0.5%. Also, we identified two less intense and broad peak at 0.24nm and 0.216nm that can be associeted with cubic structure of Be_2C. The C-Al samples on glass are suitable for crystalline structure determination and we determine for aluminum a lattice parameters about 4.09Å using classical analysis and about 4.07 Å Cohen methods[16].

TEM image of amorphous W-CFCs is shown in figure 3. We use a FFT filter to improve image contrast, by selecting a band pass filter in Fourier space and substract the resulted image from original.

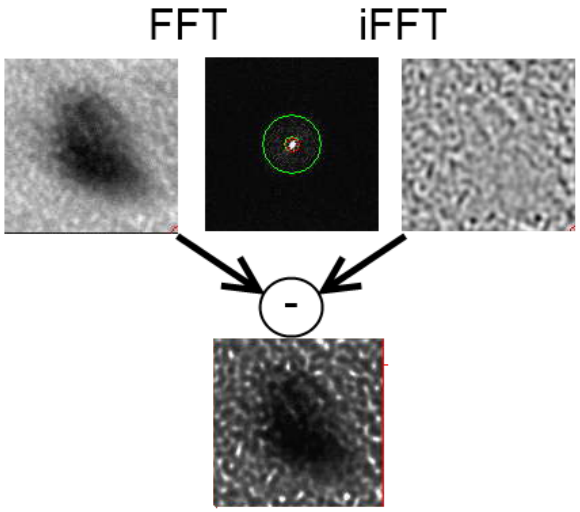

Fig. 3. TEM images of W-CFCs.

The comparative studies for invastigated structures are difficult to perform due to a lage number of parameter (geometrical, chemical, physical) that influence the final properties of nanostructures. So we addopt a modeling and simulating technique to generate and compare structures with same geometrical futures. For this task we use gbmaker and QSTEM for modeling nanostructure and simulate TEM images, and SRIM to evaluate the response of generated structure under ions bombardements.

3. Results and discussions

The comparative studies was performs on simulated images generate by ***QSTEM*** [qstem] based on models builds by ***gbmaker***[gbmaker] application. The gbmaker was recompiled in CYGWIN, initial application do not have W atom physical properties (mass, atom radius, etc.). We build two configurations of thin films: for successive deposition of carbon and metals, and mixed deposition. The real C-W system has 400nm thickness, and 200nm C + 200nm W, more than 1000000 atoms, that are very large number for usual PC system. To build these models we keep same concentration of metals and carbon for each of them. The thickness of thin films was 40nm in both configuration, and surface was keep low (2x2nm) to reduce number of atoms in generated films. These configurations keep the number of generated structure under 10000 atoms. We try to evaluate and compare C-Be and C-Al in same conditions, and we generate a 2x2x40nm structures . The efficient mode to compare simulated images is to calculate Michelson contrast [Michelson] and observe its evolutions. Michelson contrast is given by:

$$C_M = \frac{I_{max} - I_{min}}{I_{max} + I_{min}}$$

In some of the simulated images we encounter $C_M = 1$, case with maximum intensity for byte encoded image being 255 and minimum at 0. Those cases are difficult to compare. To avoid this situation we estimate maximum and minimum intensities from image histogram that will be closed to a normal distribution, and take values for intensities as:

$$I_{\substack{max \\ min}} = I_{peak} \pm SD$$

using same surface area from each image. I_{peak} and SD represent the peak of histogram and SD standard deviation. Using the second equation, Michelson contrast will be:

$$C_M = \frac{SD}{I_{peak}}$$

The obtained values are graphical represented as function of variation parameters, thickness and sample. The Fig. 4 show typical histogram obtained from C-W mixed sample, with I_{peak} and SD representation.

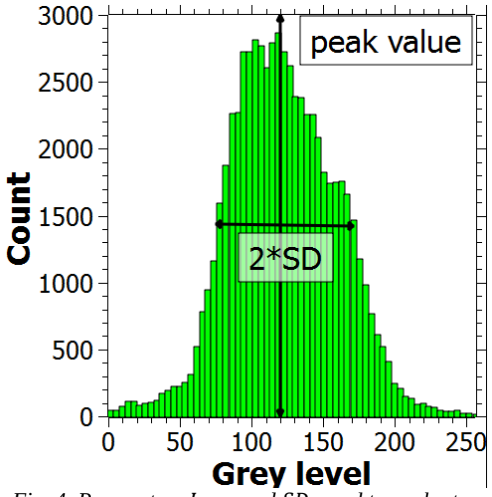

Fig. 4. Parameters I_{peak} and SD used to evaluate Michelson contrast in composite thin films

The C-W three dimensional models are shown in Fig. 5.

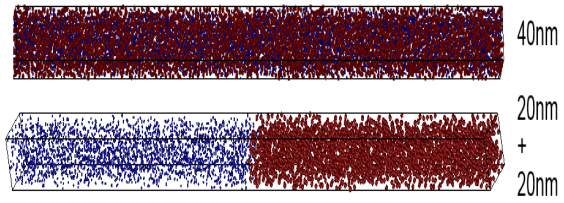

Fig. 5. 3d View of generated models.

For ions interaction we use SRIM to evaluate range of hydrogen H(^{1}H), deuterium D(^{2}H), tritium T(^{3}H) ions in our systems (Fig. 6, 7). The energies of ions were varied from 1ev to 30eV, were we found maximum range for 400 nm C-Al and C-Be nanostructured films. SRIM application is a group of program that calculate stopping power and range of ions in materials using quantum mechanical treatments of ion-atom collisions [13]. Using SRIM interface we build our system using capacities of application to define complex target. One notes that successive nanostructure is more accurate from geometrical point of view. The mixed nanostructure are only approximate generate, but we can keep the number of atoms equal to calculated number for our generated models. In this case we use a 1/1 ratio for all situation.

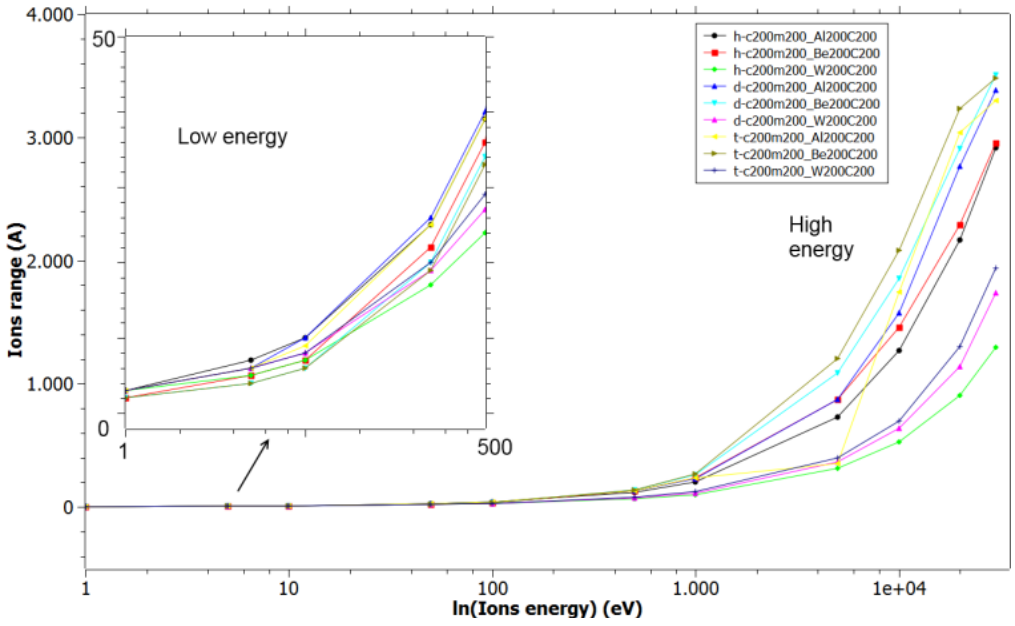

Fig. 6. Stopping range for successive layers

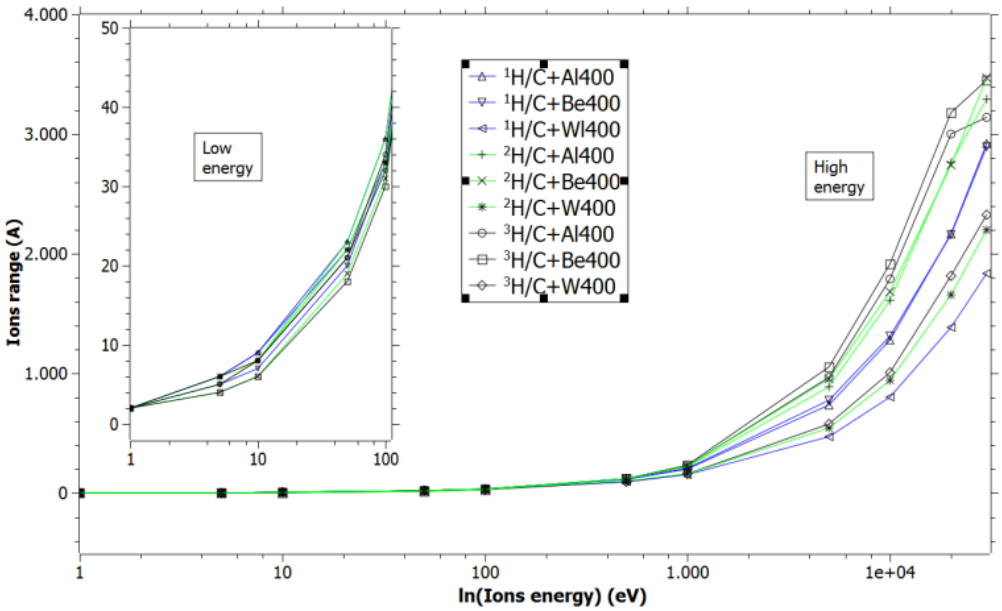

Fig. 7. Stopping range for mixed structure.

The energy of defects apparition are close for Be and Al, between 500 and 1500ev. Values of ions energies, when vacancies are produced in materials by incident ions, are shown in table 2 (SC – successive configuration, MC – mixed configuration).

Table 1. Parameters for generate models in gbmaker.

Setup	Parameter	C	Al	Be	W
	Atom radius(Å)	0.73 sp^2 0.77 sp^3	1.18	0.9	1.2
SC	C(atoms/ $Å^3$)	0.01 sp^3 0.02 sp^2	0.03	0.03	0.03
MC	C(atoms/ $Å^3$)	0.02 sp^3 0.06 sp^2	0.06	0.07	0.06
	Cryst phase Rmin(Å), Density (atoms/ $Å^3$)	Cub[13] Hex[13] 1.54d, 1.83g 0.176, 0.114	Cub [16] 2.338 0.06	Hex [15] 1.98 0.32	Cub [14] 3.16 0.06

Table 2. Ions energies threshold for vacancies produced

Ions	H(eV)		D(eV)		T(eV)	
	SC	MC	SC	MC	SC	MC
Al-CFCs	725	854	715	850	900	1050
Be-CFCs	715	800	700	785	805	975
W-CFCs	1150	1220	1210	1250	1300	1300

Behavior of Al-CFCs and Be-CFCs are close as we can see in case of H and D ions and mixed configuration.

Models are generated with gbmaker with following parameters for special framework using a random distribution. Concentration was calculated assume that r_{min} in model will be the half of minimum distance between atoms in unit cell of crystalline phase of each element, as shown in table 1. For carbon, we consider carbon hybridization with ratio 70% sp^2 and 30%sp^3. We calculate relative concentration using a weighted formula for mixed models (1:1 ratio), and calculated from Rmin, as implemented in gbmaker ($\rho = \sqrt{\frac{15}{144}} \cdot \frac{1}{R_{min}^3}$), for successive models. Also we keep in mind that gbmaker work with 4 atoms for each unit cell for amorphous and special structure.

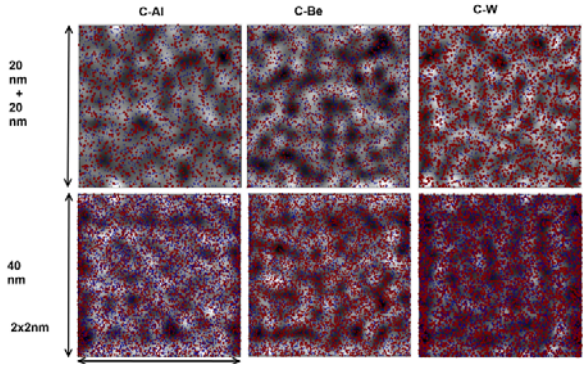

Fig. 8. Simulated images superimposed by generated models.

We observe a low density in case of successive models. As we defined a radius for each atom, in the input file for gbmaker, numbers of atoms are randomly distributed, with minimum distance between atoms at twice of atoms radius. In successive case the radius will be $2R_M$ for metal layers, and $2R_C$ for carbon layer.

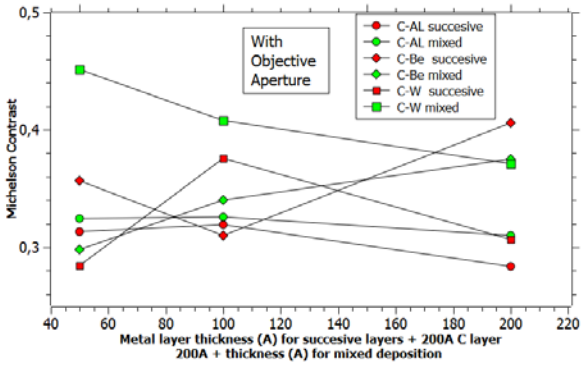

Fig. 9. Michelson contrast from images simulated with 15mrad objective aperture.

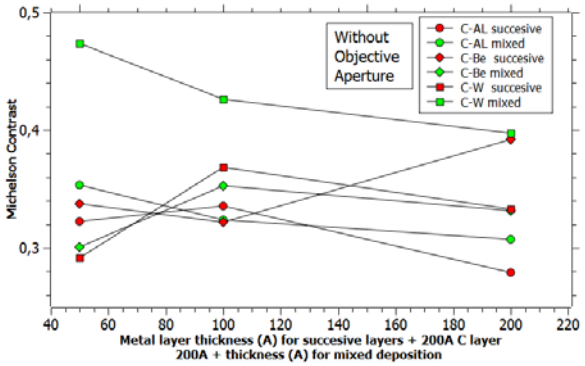

Fig. 10. Michelson contrast from images simulated without objective aperture.

The effect of aperture objective is very weak in these configurations, but we can remark a slight change in case of Al-CFCs and Be-CFCs. Both configurations, SC and MC, exhibit a mean contrast around 0.35. As we expect W-CFCs are greater for MC configuration, where W atoms are distributed along total volume of thin film.

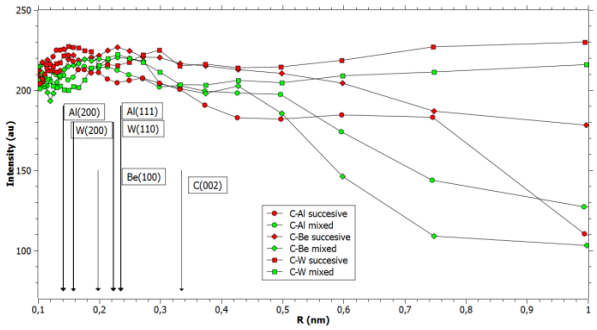

Fig. 11. Electron diffraction profile with first lines of crystalline phase marked.

Electron diffraction pattern was calculated using Weickenmeier-Kohl parametrization [20] for electron scattering factor.

4. Conclusions

TVA was used succesfully for hydrogen free carbon film deposition, as well as composite carbon based films from two different sources, ignited simultaneously. Their characteristics are presumed to be similar with the future resulting inner wall surface after the thermo-nuclear plasma exposure inside ITER.

The C-W films were identified as a nanocrystals complex (5 nm average diameter) surrounded by amorphous structures with a strong graphitization tendency, allowing the creating of adherent and wear resistant films.

XPS analysis proved beryllium-carbide formation inside the composite samples. The presence of the Be_2C inside the whole film was noticed. Comparative study of the TDS data was performed in order to study the behavior of deuterium desorption inside the implanted samples. For the samples implanted at room temperature, a pronounced peak around a sample temperature of 150^{o}C is revealed and a low intensity peak around 550^{o}C.

The results obtained have a great impact on the development of advanced material as well as expanding the technologically important field of interface science where the control of the film-substrate interface would be critical.

The crystalline structure of film is confirmed to be cubic for aluminium phase, and hexagonal for partial graphitized carbon. The main part of carbon is amorphous, reveal by electron diffraction pattern. The lattice parameter for aluminium phase are greater than referenced one, determined with ~1.2% relative error by classical method and ~0.7% by Cohen with modified Nelson-Riley method.

The C-Al film exhibits the same future like C-Be films, regarding tribological properties with low friction coefficient. The obtained film has uniformly thickness adherent and wear resistant films. Carbon rich sample show friction coefficient as the same size like C-Be films, 3-5 times smaller than substrate. Aluminium rich film shows a larger friction coefficient, about half reported to the substrate friction coefficient.

Behavior of Al-CFCs and Be-CFCs under ions bombardments are similar, in case of H and D ions and mixed configurations.

Compared contrast from simulated TEM images are close to 0.35 for Al-CFCs and Be-CFCs in both configuration, successive and mixed. W-CFCs exhibit a better contrast for mixed configuration, with value for Michelson contrast over 0.4.

Acknowledgements

The paper was supported by a grant of the Romanian National Authority for Scientific Research, CNDI-

UEFISCDI, project number 160/2012, PN-II-PT-PCCA-2011-3.2-1453

References

[1] Z. Yang, Q. Xu, J. Liao, Q.Li, G-H. Lu, G-N. Luo, Nucl. Instrum. Meth. B **267**, 3144 (2009)
[2] D. Borodin, R. Doerner, D. Nishijima, A. Kirschner, A. Kreter, D. Matveev, A. Galonska, V. Philipps, J. Nucl. Mat. **415**, S219 (2011)
[3] A. Lasa, C. Bjorkas, K. Vortler, K. Nordlund, J. Nucl. Mat. **429**, 284 (2012)
[4] D. Aquaro, M. Di Prinzio, Fusion Eng. Des. **82**, 1681 (2007).
[5] V. Ciupina, I. Morjan, C. P. Lungu, R. Vladoiu, G. Prodan, M. Prodan, V. Zarovschi, C. Porosnicu, I. M. Stanescu, M. Contulov, A. Mandes, V. Dinca K. Sugiyama, Proc. SPIE 8104, 810411 (2011); DOI: 10.1117/12.892198
[6] V. Ciupina, C. Lungu, R. Vladoiu, D-T. Epure, G. Prodan, C. Porosnicu, M. Prodan, I-M. Stanescu, M. Contulov, A. Mandes, V. Dinca, V. Zarovschi, Proc. SPIE 8465, 930443 (2012); DOI:10.1117/12.930443
[7]CAS#7440-41-7 http://www.first.ethz.ch/infrastructure/Chemicals/Salts_solids/MSDS_Be.pdf
[8] Canadian Centre for Occupational Health & Safety site
[9] CAS #7429-90-5
[10] V. Ciupina, I. G. Morjan, R. Alexandrescu, et al., Proceedings of SPIE Vol. **7764**, 77640O (2010)
[11] R. Vladoiu, V. Ciupina, C. Surdu-Bob, C.P. Lungu, J. Janik, J.D. Skalny, V. Bursikova, J. Bursik, G. Musa, J. Optoelectron .Adv. Mater. **9**(4), 862 (2007).
[12] G. Musa, I. Mustata, V. Ciupina, R. Vladoiu, G. Prodan, E. Vasile, H. Ehrich, Diamond and Related Materials **13**, 1398 (2004).
[13] R. W. G. Wyckoff , Second edition. Interscience Publishers, New York, New York Crystal Structures 1, 7 (1963) =.
[14] R.W.G. Wyckoff, [Crystal Structures], sec. ed., vol. 1, John Wiley & Sons, New York & London, 27-28 (1963);
[15] R.W.G. Wyckoff, [Crystal Structures], sec. ed., vol. 1, John Wiley & Sons, New York & London, 9-11 (1963);
[16] R.W.G. Wyckoff, [Crystal Structures], sec. ed., vol. 1, John Wiley & Sons, New York & London, 239-444 (1963);
[17] C.T. Koch, "Determination of Core Structure Periodicity and Point Defect Density along Dislocations", Arizona Stat Univ. (2002)
[18] Michelson, A. *Studies in Optics*. U. of Chicago Press. (1927).
[19] "***SRIM - The Stopping and Range of Ions in Solids***", by J. F. Ziegler and J. P. Biersack in 1985
[20] A. Weickenmeier, H. Kohl, "Computation of Absorptive Form Factor for High-Energy Electron Diffraction", Acta Crystall. A **47**, 590 (1991).

*Corresponding author: rvladoiu@univ-ovidius.ro